JOURNAL OF GUIDANCE, CONTROL, AND DYNAMICS
Vol. 19, No. 4, July–August 1996

Motion Control of Free-Floating Variable Geometry Truss Part 1: Kinematics

Shengyang Huang
Toyota Technological Institute, Tempaku, Nagoya 468, Japan
M. C. Natori
Institute of Space and Astronautical Science, Sagamihara 229, Japan
and
Kohichi Miura
Nihon University, Narashinodai, Funabashi 274, Japan

A variable geometry truss is representative of adaptive structures, whose shape can be intentionally altered through shortening or lengthening its adjustable length members, and so has gained some applications in space engineering including space robots, payload isolation, and so on. A new application of variable geometry trusses is proposed, where variable geometry trusses, as components of some larger space structure, might be expected to construct themselves through their adaptivity. Unlike applications such as space manipulators where a variable geometry truss is considered to be fixed on some platform, in this case a variable geometry truss is free floating in three-dimensional space. To this end, the approach on controlling the motion of a free-floating variable geometry truss is discussed from the standpoint of kinematics. Through taking into account the conservation of momentum of the structural system, a family of compact equations is provided to describe the geometry and motion of free-floating variable geometry trusses. Based on the centroid displacement vector *d* of a variable geometry truss bay, a group of pseudolinear equations for determining the geometry shape of a free-floating variable geometry truss is obtained. With a simple representation for the angular velocity of a variable geometry truss bay, obtained here, the orientation control for the bay's working plane is made possible. Finally, a simulation is performed to demonstrate the validity of the derived equations.

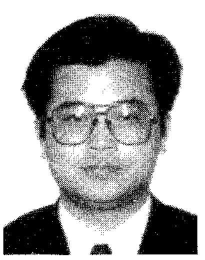

Shenyang Huang received his B.Eng. degree in applied mechanics from Huazhong University of Science and Technology, China, in 1983 and the M.Eng. and Ph.D. degrees, both in computational mechanics, from Dalian University of Technology, China, in 1983 and 1989, respectively. In 1990, he joined the Dalian University of Technology as a lecturer. From January 1991 to June 1994, he was a foreign research fellow in spacecraft engineering at the Institute of Space and Astronautical Science, Japan. Since July 1994, he has been an invited research fellow at the Intelligent System Laboratory of the Toyota Technological Institute, Japan. His research interests include engineering database systems, knowledge-based systems, object-oriented approaches, distributed autonomous systems, and motion controls of intelligent adaptive structures.

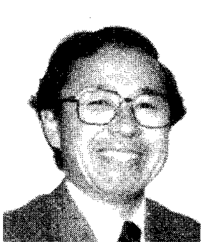

M. C. Natori received his B.S., M.S., and D.Eng. degrees from the University of Tokyo, Japan, in 1967, 1969, and 1972, respectively. He worked at the Institute of Space and Aeronautical Science of the University of Tokyo and joined the faculty of the Institute of Space and Astronautical Science in 1983. Currently, he is a professor of spacecraft engineering at the Institute of Space and Astronautical Science and also at the University of Tokyo. His major research fields are space structures engineering, structural dynamics and control, aeroelasticity, and science on form. Dr. Natori is currently an experiments manager of the Space Flyer Unit, a manager of the MUSES-B antenna structure development for the Japanese space VLBI program, and a cochair of the Department of Architecture at the International Space University. He is a member of the Structures Technical Committee of the AIAA, the Adaptive Structures Technical Committee of the American Society of Mechanical Engineers, the Japan Society for Aeronautical and Space Sciences, the Japan Society of Mechanical Engineers, and the Society of Science on Form (Editorial Board). He is also a member of the editorial board of two journals: *Smart Materials and Structures* and *Journal of Intelligent Material Systems and Structures*.

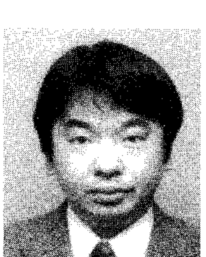

Kohichi Miura received his B.Eng. and M.Eng. degrees, both in mechanical engineering, from Nihon University, Japan, in 1980 and 1982, respectively. Since 1985, he has been a research associate at the Department of Junior College, Nihon University. His research interests include dynamics and control of intelligent adaptive structures.

Received April 20, 1994; revision received Feb. 19, 1996; accepted for publication Feb. 26, 1996.

Nomenclature

$A_{i,k}$ = project matrix that maps the differentiation of vector $\boldsymbol{d}$ of the kth bay to the center-of-mass velocity of the ith passive plane
$\boldsymbol{a}_i$ = position vector of the ith apex ($i = 0, 1, 2$) of a triangle stretched from its centroid
$\boldsymbol{D}_b, \boldsymbol{D}_i$ = bay transformation matrix, namely, the transformation matrix of the top plane of a bay with respect to its bottom plane
$\boldsymbol{d}$ or $\boldsymbol{d}_i$ = centroid displacement vector that stretches between the centroids of bottom and top triangles
$\boldsymbol{g}_b$ = center-of-mass vector of a bay
$\boldsymbol{g}_n$ = center-of-mass vector of a bay member
$\boldsymbol{I}$ = identity matrix
$\boldsymbol{I}_n$ = inertial moment of a passive member of a bay
l = length of members of a variable geometry truss (VGT)
l_i, l_n = length of a member of a VGT including the members of the middle triangular batten
$\boldsymbol{l}_j, \boldsymbol{l}_n$ = direction vector of a member of a bay
M_b = total mass of a bay
M_G = total mass of the overall VGT structure
m_n = mass of a bay member
$\boldsymbol{n}_1$ = normal vector of the bottom plane of a bay
$\boldsymbol{n}_2$ = normal vector of the top plane of a bay
$\boldsymbol{P}$ = project matrix that maps the differentiation of vector $\boldsymbol{d}$ to the angular velocity of the top plane of a bay with respect to its bottom plane
$\boldsymbol{p}_G$ = center-of-mass vector of the whole structure
$\boldsymbol{p}_i$ = center-of-mass vector of the ith passive plane in an inertial coordinate system
$\boldsymbol{R}_i$ = project matrix that maps the differentiation of vector $\boldsymbol{d}$ to the ith nodal velocity that is defined in the bay reference frame
r = altitude of the identical equilateral triangle with the side-length of l, $(\sqrt{3}/2)l$
$\boldsymbol{r}_i$ = position vector of an apex of a bay with respect to the origin of an inertial coordinate system
$\boldsymbol{r}'_i$ = position vector of an apex of a bay with respect to the origin of the bay coordinate system
$\boldsymbol{t}_j$ = center-of-mass vector stretched from the top plane of the ith bay to the center of mass of the middle plane of the same bay, and defined in the bay coordinate system
$\tilde{\boldsymbol{v}}$ = skew matrix of vector $\boldsymbol{v}$
Δ = offset of hinge
ρ = mass ratio of a logic VGT bay to the total mass of the structure
$\boldsymbol{\Phi}_0$ = vector expression of the orientations of the free endplane of a free-floating VGT
ω or ω_j = angular velocity of the top plane with respect to the bottom plane within a bay, and defined in the bay coordinate system

Superscript

A = inertial coordinate system where a vector is defined or to which a project matrix maps a vector

Subscripts

i = layer number within a bay for vector $\boldsymbol{r}$ and matrix $\boldsymbol{R}$
A = inertial coordinate system with respect to which a passive plane rotates, used for ω and $\boldsymbol{D}$

I. Introduction

THE concept of an adaptive structure is new to the field of space structures.[1,2] It describes a structure whose geometrical configuration and physical characteristics can be intentionally varied to meet mission requirements and space environmental conditions. Adaptive truss structures are representative of those various adaptive structures. An octahedral variable geometry truss (VGT), as an adaptive structure, was first proposed by Miura and Furuya,[3] whose fundamental module was composed of a pair of lateral triangular battens and six diagonal members. Two adjacent modules, which share one lateral batten, comprise a repeating unit of the truss. Then, the overall structure is formed through the repetition of units in a longitudinal direction (Fig. 1). By altering the length of members of the lateral batten, which are equipped with actuators and encoders, various configuration changes of the structure could be achieved.

There have been many studies on the geometry of VGTs. Miura and Furuya[3] suggested a group of formulations to describe the geometry of a simplified VGT in which three angle parameters are used to express the nonlinear relationships of a VGT. Recently the kinematics for a generalized VGT unit was also proposed.[4] Naccarato and Hughes[5] presented the curve kinematics of VGTs, based on the inverse kinematics of a so-called VGT bay, to achieve their motion controls when they are used as space robots. Because adaptive trusses are usually equipped with a large number of actuators, they can offer more dexterity than conventional robot arms and so have found several applications in space robots, serpentine manipulators, payload isolation, and so on.

An alternate application for a VGT in which VGTs are used as the components of a larger space structure might be explored. In this case, a VGT will construct itself into another structure through its ability to change its shape. Figure 2 shows an example of such an application where two endplanes of a VGT are to be docked with other components, in which case the redundant actuators could be employed to meet extra requirements such as some needed change of shape, obstacle avoidance, etc., because of the construction environment of a large space structure. Basically, a VGT in this case is a free-floating structure in three-dimensional space so that a docking procedure is carried out without any base-fixed endplane. Obviously, this is a different case from the docking of space manipulators of VGTs. The key issue here is that the mutual reaction of the two endplanes must be taken into account, which means the kinematics and control method for the docking treatment of VGTs with one base-fixed endplane are no longer suitable. Concerning the control method and kinematics of a free-floating multibody system, Umetani and Yoshida[6] derived a generalized form of the Jacobian matrix by introducing the conservation law of momentum to represent the dynamics of a free-floating system. Based on the concept of the so-called generalized Jacobian matrix, the docking of a free-floating structure in two-dimensional space was treated.[7] However, only the link structure that is inherently a two-dimensional structure system has been dealt with to date.

In this paper, the authors present a family of compact formulations concerning the kinematics and control of a free-floating VGT in the three-dimensional space. By taking the conservation of momentum of the structure system into account, a group of pseudo-linear equations for the geometric shape of the structure is established in terms of vector $\boldsymbol{d}$, the centroid displacement vector of a bay proposed in Ref. 5. Moreover, the computational formulations

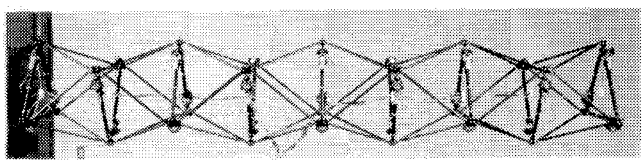

Fig. 1 Variable geometry truss.

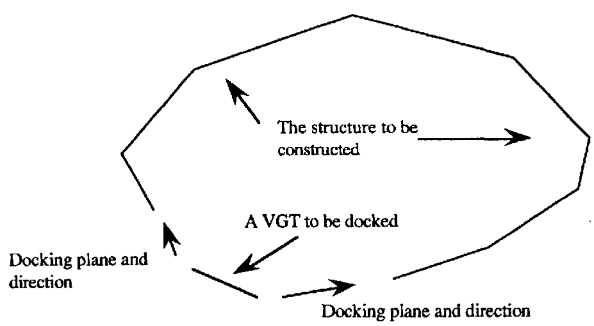

Fig. 2 Alternate application of VGTs.

of angular momentum are also expressed with vector $\boldsymbol{d}$ of a bay. Based on the simple form of the angular velocity of a bay derived in this paper, a compact control equation for the orientation of the docking plane is obtained. To demonstrate the validity of the derived equations and with the objective of facilitating space construction, a simulation is performed and the simulation results are provided.

II. Kinematics of a VGT Bay

A bay is a truss unit that is composed of two VGT modules[3] with the assumption that both the base and the top lateral trusses are identical equilateral triangles and whose members always keep the same length as all of the diagonal members, with only the middle lateral truss being able to vary the length of its members. (See Fig. 3.) A geometric model of one VGT bay is shown in Fig. 3.

It needs to be made clear that all of the geometric vectors within a bay are represented in the bay coordinate system that is mounted on the bottom plane and is defined in Fig. 3b. For the sake of simplicity, the three planes (bottom, middle, and top planes shown as Fig. 3) of a bay are further divided into seven layers sequentially from the bottom to the top, which are numbered from 0 to 6. Each layer relates a triangle with nodes (0, 1, 2).

A. Geometry of One Bay

1. Control Variable of a VGT Bay

Instead of using the geometric representation of a VGT bay suggested in Ref. 3, the vector $\boldsymbol{d}$ proposed in Ref. 5, which is the centroid displacement vector that stretches between the centroids of the bottom and top triangles, is selected to be the control variable of a bay. This treatment implies avoiding the kinematics to directly achieve the inverse kinematics of a bay.

2. Rotation Transformation Matrix

Because of the symmetry of a VGT bay (Fig. 3a), the rotation transformation relating the bottom plane to the top plane, which is defined to be the bay transformation matrix, becomes (also see Ref. 5)

$$\boldsymbol{D}_b(\varphi, \boldsymbol{v}) = \cos\varphi \boldsymbol{I} + (1 - \cos\varphi)\boldsymbol{v}\boldsymbol{v}^T - \sin\varphi\tilde{\boldsymbol{v}} \tag{1}$$

where

$$\cos\varphi = \boldsymbol{n}_1^T\boldsymbol{n}_2 \tag{1a}$$

$$\boldsymbol{n}_2 = [2(\boldsymbol{d}\boldsymbol{d}^T/\boldsymbol{d}^T\boldsymbol{d}) - \boldsymbol{I}]\boldsymbol{n}_1 \tag{1b}$$

$$\boldsymbol{v} = \frac{\boldsymbol{n}_2 \times \boldsymbol{n}_1}{\|\boldsymbol{n}_2 \times \boldsymbol{n}_1\|} = \frac{1}{\|\boldsymbol{d} \times \boldsymbol{n}_1\|}\tilde{\boldsymbol{d}}\boldsymbol{n}_1 \tag{1c}$$

3. Apices in the Middle Plane

The position of an apex on the second layer (Fig. 4) is given by

$$_2\boldsymbol{r}_i = \boldsymbol{p}_{b-1} + {_2\boldsymbol{r}'_i} \qquad i \in (0, 1, 2) \tag{2}$$

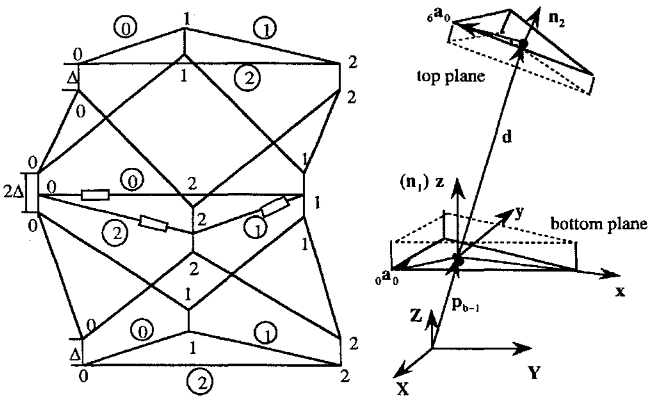

a) Bay

b) Bay coordinate system

Fig. 3 Geometrical model of a VGT bay.

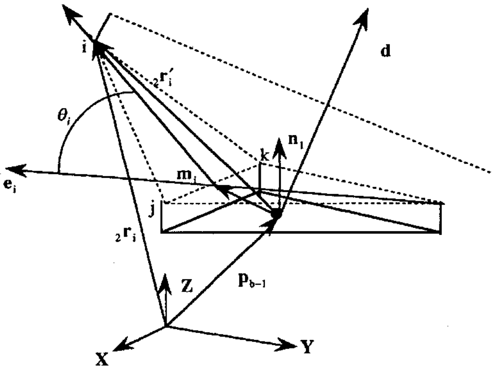

Fig. 4 Apex of the second layer.

where

$$_2\boldsymbol{r}'_i = \boldsymbol{m}_i + r\cos\theta_i\boldsymbol{e}_i + r\sin\theta_i\boldsymbol{n}_1 \tag{2a}$$

$$\theta_i = \arcsin(B_i/A_i) - \alpha_i \tag{2b}$$

$$tg\alpha_i = \boldsymbol{e}_i^T\boldsymbol{d}/\boldsymbol{n}_1\boldsymbol{d} \tag{2c}$$

$$A_i = r\sqrt{\left(\boldsymbol{e}_i^T\boldsymbol{d}\right)^2 + (\boldsymbol{n}_1\boldsymbol{d})^2} \tag{2d}$$

$$B_i = \gamma\boldsymbol{d}^T\boldsymbol{d} - \boldsymbol{m}_i^T\boldsymbol{d} \tag{2e}$$

$$\gamma = \tfrac{1}{2} - (\Delta/\|\boldsymbol{d}\|) \tag{2f}$$

where $\boldsymbol{m}_i$ is the position vector stretching from the middle point of the side (j, k) to the origin of bay coordinate system and $\boldsymbol{e}_i$ is the direction vector perpendicular to the side (j, k) on the 1st layer.

Then the remaining apices in the middle plane can be represented by

$$_j\boldsymbol{r}'_i = {_{j-1}\boldsymbol{r}'_i} + \Delta(\boldsymbol{d}/\|\boldsymbol{d}\|) \qquad j \in (3, 4), \qquad i \in (0, 1, 2) \tag{2g}$$

4. Apices of the Top Plane

With vector $\boldsymbol{d}$ and transformation matrix $\boldsymbol{D}_b$, an apex vector in the top plane with respect to the origin of the bay coordinate system can be easily obtained (Fig. 3b):

$$_j\boldsymbol{r}'_i = \boldsymbol{d} + \boldsymbol{D}_{b\,j}\boldsymbol{a}_i - \lambda_j\Delta\boldsymbol{n}_2$$

$$j \in (5, 6), \qquad i \in (0, 1, 2), \qquad \lambda_j = \begin{cases} 1, & j = 5 \\ 0, & j = 6 \end{cases} \tag{3}$$

B. Differentiation Within a Bay

To achieve motion control of a VGT, the first-order differentiation plays a key role. Here, the key issue is that we can use vector $\boldsymbol{d}$ to represent the various differentiating variables within a VGT bay.

1. Angular Velocity of a Bay with Respect to the Bottom Plane

To handle the orientation of the top plane of a bay, the concept of relative angular velocity of a bay is introduced, and is defined to be[8,9]

$$\tilde{\omega} = \dot{\boldsymbol{D}}_b\boldsymbol{D}_b^T \tag{4}$$

Using Eq. (1) and after a tedious derivation (see Appendix), ω can be solved and represented as follows:

$$\omega = (2/\boldsymbol{d}^T\boldsymbol{d})(\boldsymbol{d} \times \dot{\boldsymbol{d}}) \tag{5}$$

Furthermore, we can write it in the form of a matrix

$$\omega = \boldsymbol{P}\dot{\boldsymbol{d}} \tag{6}$$

$$\boldsymbol{P} = (2/\boldsymbol{d}^T\boldsymbol{d})\tilde{\boldsymbol{d}} \tag{6a}$$

2. Apical Velocities of the Middle Plane

Differentiating Eq. (2a), we have the expressions

$$\frac{\mathrm{d}_2 \boldsymbol{r}'_i}{\mathrm{d}t} = {}_2\boldsymbol{R}_i \dot{\boldsymbol{d}} \qquad i \in (0, 1, 2) \tag{7}$$

$${}_2\boldsymbol{R}_i = \boldsymbol{q}_i \boldsymbol{t}_i^T \tag{7a}$$

$$\boldsymbol{t}_i = \frac{1}{A_i \cos\phi_i}\left[\left(\frac{1}{2} + \gamma\right)\boldsymbol{d} - {}_2\boldsymbol{r}'_i\right] \tag{7b}$$

$$\phi_i = \arcsin(B_i / A_i) \tag{7c}$$

$$\boldsymbol{q}_i = r\cos\theta_i \boldsymbol{n}_1 - r\sin\theta_i \boldsymbol{e}_i \tag{7d}$$

Similarly, we obtain the following equations from Eq. (2g):

$$\frac{\mathrm{d}_j \boldsymbol{r}'_i}{\mathrm{d}t} = {}_j\boldsymbol{R}_i \dot{\boldsymbol{d}} \qquad j \in (3, 4), \qquad i \in (0, 1, 2) \tag{8}$$

$${}_j\boldsymbol{R}_i = {}_{j-1}\boldsymbol{R}_i + (\Delta/\|\boldsymbol{d}\|)[\boldsymbol{I} - (\boldsymbol{d}\boldsymbol{d}^T/\boldsymbol{d}^T\boldsymbol{d})] \tag{8a}$$

3. Apical Velocities of the Top Plane

An apical velocity of the top plane can be solved by directly differentiating Eq. (3), whose expression is given in the same way as Eqs. (7) and (8) with a different representation for matrix $\boldsymbol{R}$, where matrix $\boldsymbol{R}$ is given by

$${}_j\boldsymbol{R}_i = \boldsymbol{I} - (\boldsymbol{D}_{b\,j}\boldsymbol{a}_i - \lambda_j \Delta \boldsymbol{n}_2)\boldsymbol{P}$$

$$j \in (5, 6), \qquad i \in (0, 1, 2), \qquad \lambda_j = \begin{cases} 1, & j = 5 \\ 0, & j = 6 \end{cases} \tag{9}$$

4. Determination of Actuator Speeds

With control vector $\boldsymbol{d}$ of a bay, the speeds of actual actuators, namely, the change rate of three variable length members in the middle plane, can be easily obtained. Express the current lengths of these three length-variable members with a vector $\boldsymbol{L} = \{l_i\}$, $i \in (0, 1, 2)$, and let $\boldsymbol{l}_i\,(i = 0, 1, 2)$ be the direction vector of the ith member in the bay reference frame. Note that $\dot{l}_0 = \boldsymbol{l}_0 \cdot ({}_3\dot{\boldsymbol{r}}'_1 - {}_3\dot{\boldsymbol{r}}'_0)$, where $\boldsymbol{l}_0 = ({}_3\boldsymbol{r}'_1 - {}_3\boldsymbol{r}'_0)/l_0$ (Fig. 3a) and ${}_3\dot{\boldsymbol{r}}'_j\,(j = 0, 1)$ can be solved by Eq. (8). The values of the other two actuators can be obtained similarly. Ultimately we have the expression

$$\dot{\boldsymbol{L}} = \begin{bmatrix} \boldsymbol{l}_0({}_3\boldsymbol{R}_1 - {}_3\boldsymbol{R}_0) \\ \boldsymbol{l}_1({}_3\boldsymbol{R}_2 - {}_3\boldsymbol{R}_4) \\ \boldsymbol{l}_2({}_3\boldsymbol{R}_0 - {}_3\boldsymbol{R}_2) \end{bmatrix} \dot{\boldsymbol{d}} \tag{10}$$

III. Motion Equations of a Free-Floating Structure

A. Chain Model of the Structure

The structure shown in Fig. 1 is characterized by a chain of bays. (See Fig. 5.) However, a problem arises when the bay model as described is assembled into the structure as a component because the two adjacent bays share a common triangular batten. To eliminate this construction redundancy, a logic bay and a virtual bay model are introduced.

A logic bay, slightly different in construction from the bay as shown in Fig. 3, consists of two lateral triangular trusses (a middle plane and a top plane seen in Fig. 3), a virtual bottom plane that has no real constructing members and that will be replaced by the top plane of some other logic bay when the structure is constructed, six diagonal members to connect two lateral trusses, six diagonal members to anchor the logic bay to the virtual bottom plane, and all corresponding hinges. Briefly, a logic bay embodies two real planes, a virtual plane, and 12 diagonal members. For the sake of complete description of the structure, the concept of a so-called virtual bay is introduced, which is just composed of a lateral triangular truss with no actuators equipped at its top plane.

A plane that has no changeable member may be called a passive plane. Similarly, a plane equipped with actuators is called an active plane. Moreover, to set up a proper model to describe the motion features of such a structure, we label all bays by $0, 1, 2, \ldots, n$,

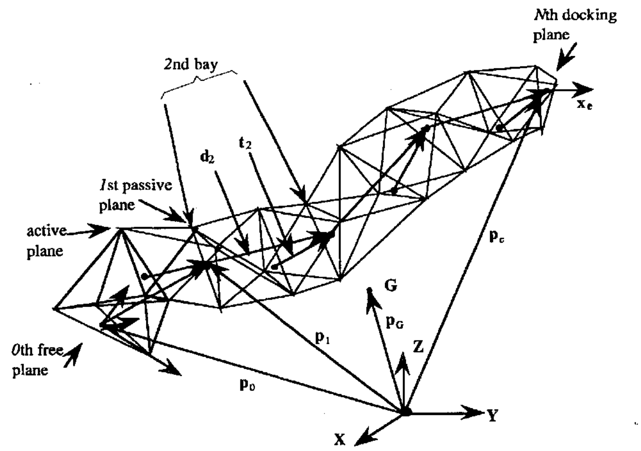

Fig. 5 Chain model of the structure.

where 0 indicates the virtual bay. Accordingly, all of the passive planes that correspond to the top planes of bays are numbered with $0, 1, 2, \ldots, n$. If we set the XY plane of an inertial coordinate system to be the -1st passive plane to observe the motion of the structure, it is easy to find that rotation of the ith passive plane is achieved through the consecutive rotation of each plane from the 0th to it.

B. Rotation of a Passive Plane

Letting ${}_A\boldsymbol{D}_i$ be the transformation matrix of the ith bay with respect to the inertial coordinate system, and letting the bay transformation matrix of the ith bay be $\boldsymbol{D}_i$ [see $\boldsymbol{D}_b$ in Eq. (1)], we can write

$$\begin{gathered} {}_A\boldsymbol{D}_i = \boldsymbol{D}_0\boldsymbol{D}_1 \cdots \boldsymbol{D}_i = \prod_{j=0}^{i} \boldsymbol{D}_j \\ \boldsymbol{D}_j^{-1} = \boldsymbol{D}_j^T \end{gathered} \tag{11}$$

Similar to Eq. (4), the angular velocity of the ith plane with respect to the inertial coordinate system is defined to be

$${}^A_A\tilde{\omega}_i = {}_A\dot{\boldsymbol{D}}_i\,{}_A\boldsymbol{D}_i^T \tag{12}$$

where the superscript A of ω indicates that ω is defined in the inertial coordinate system and the subscript A shows that the rotation is with respect to the -1st plane, namely, the inertial coordinate system.

After differentiating Eq. (11), we can arrive at

$${}^A_A\tilde{\omega}_i = {}^A\tilde{\omega}_0 + \sum_{j=1}^{i} {}_A\boldsymbol{D}_{j-1}\tilde{\omega}_j\,{}_A\boldsymbol{D}_{j-1}^T \tag{13}$$

where ω_j is the angular velocity of the top plane of the jth bay with respect to the bay coordinate system, which can be obtained from Eq. (5) or (6). Let

$${}^A\tilde{\omega}_j = {}_A\boldsymbol{D}_{j-1}\tilde{\omega}_j\,{}_A\boldsymbol{D}_{j-1}^T \tag{13a}$$

Obviously, Eq. (13a) is just the alternative expression of ω_j in the inertial coordinate system. Hence, we can rewrite Eq. (13) as

$${}^A_A\omega_i = {}^A\omega_0 + \sum_{j=1}^{i} {}^A\omega_j \tag{13b}$$

Using Eq. (6) and noting that it is easy to represent ω of the virtual bay in the same way as Eq. (6), then after rearrangement, we can rewrite Eq. (13b) into

$${}^A_A\omega_i = \boldsymbol{P}_0\dot{\boldsymbol{\Phi}}_0 + \sum_{j=1}^{i} {}^A\boldsymbol{P}_j\dot{\boldsymbol{d}}_j \tag{13c}$$

where $\boldsymbol{\Phi}_0$ stands for the orientations of a free endplane, which is expressed in the form of a vector.

C. Center-of-Mass Vector of a Passive Plane

Basically, the mass of a passive plane includes the sum of the concentrated masses of three hinges and the masses of three lateral members. Because the mass of a diagonal member of a bay can be evenly converted onto its two endpoints, a diagonal member can be viewed as null mass after adding a concentrated mass of $m/2$ to each hinge of the passive or active plane to which it is connected. Thus, the mass of a passive plane also involves the sum of the masses of three diagonal members. Letting the masses of a passive plane and an active plane be M_p^i and M_a^i, respectively, then the total mass of the structure can be obtained by summing the masses of all passive and active planes. Thus, the geometrical definition of the center of mass of structure is given by

$$M_G \boldsymbol{p}_G = \sum_{i=1}^{N} \left(M_p^i \boldsymbol{p}_i + M_a^i \boldsymbol{p}_{i,a} \right) + M_p^0 \boldsymbol{p}_0 \tag{14}$$

where N is the number of the bays that comprise the structure and $\boldsymbol{p}_{i,a}$ is the center-of-mass vector of the active plane in the ith bay. Assuming that all passive planes, all active planes, and all lateral members have same geometric and physical composition, we can define ρ as

$$\rho = \rho_j = \rho_a^j + \rho_p^j = \left(M_a^j / M_G \right) + \left(M_p^j / M_G \right) \qquad (0 < j < N)$$

$$\rho_t = \rho_N = M_p^N / M_G \tag{15}$$

$$\rho_a = \rho_a^j \qquad (0 < j \leq N)$$

and express $\boldsymbol{p}_{i,a}$ as

$$\boldsymbol{p}_{i,a} = \boldsymbol{p}_i - {}^A\boldsymbol{t}_i \qquad {}^A\boldsymbol{t}_i = {}^A\boldsymbol{d}_i - \boldsymbol{p}'_{i,a} \tag{16}$$

where $\boldsymbol{p}'_{i,a}$ is the center-of-mass vector of the active plane of the ith bay with respect to the origin of its bay coordinate system.

Note that ${}^A\boldsymbol{t}_i$, ${}^A\boldsymbol{d}_i$, $\boldsymbol{p}_{i,a}$, and $\boldsymbol{p}_i$ are all defined in the inertial coordinate system. Considering the chain feature of the structure, we can establish the following recursive formulation:

$$\boldsymbol{p}_i - \boldsymbol{p}_{i-1} = {}^A\boldsymbol{d}_i \qquad (i = 1, \ldots, N) \tag{17}$$

With Eqs. (14–17), we can obtain the following equation for the center-of-mass vector of the ith passive plane:

$$\boldsymbol{p}_i = \sum_{j=1}^{N} \left(K_{ij} {}^A\boldsymbol{d}_j + \rho_a {}^A\boldsymbol{t}_j \right) + \boldsymbol{p}_G \qquad (i = 0, \ldots, N) \tag{18}$$

where

$$K_{ij} = \begin{cases} 1 - [(N-j)\rho + \rho_t] & j \leq i \\ -[(N-j)\rho + \rho_t] & j > i \end{cases} \tag{18a}$$

D. Center-of-Mass Velocity of a Passive Plane

The center-of-mass velocity of a passive plane is a key to determining the change of shape of a free-floating structure, and to controlling its motion. Differentiating Eq. (18), upon substitution of Eq. (13c), we can obtain

$$\dot{\boldsymbol{p}}_i = \sum_{k=0}^{N-1} {}^A\boldsymbol{\omega}_k \times {}^A\boldsymbol{\pi}_{i,k} + \sum_{j=1}^{N} {}_A\boldsymbol{D}_{j-1}(K_{ij}\boldsymbol{I} + \rho_a \boldsymbol{T}_j)\dot{\boldsymbol{d}}_j \tag{19}$$

where

$${}^A\boldsymbol{\pi}_{i,k} = \sum_{j=k+1}^{N} \left(K_{ij} {}^A\boldsymbol{d}_j + \rho_a {}^A\boldsymbol{t}_j \right) \tag{20}$$

and $\boldsymbol{T}_j (j = 1, N)$ is a project matrix, which satisfies

$$\dot{\boldsymbol{t}}_j = \boldsymbol{T}_j \dot{\boldsymbol{d}}_j$$

and takes the form

$$\boldsymbol{T}_j = \boldsymbol{I} - \frac{1}{M_a} \sum_{l=0}^{2} m_l \, {}_3\boldsymbol{R}_1^j \tag{21}$$

where ${}_3\boldsymbol{R}_1^j$ is solved by Eq. (8a), m_l is the equivalent mass of each hinge, which is contributed to by the concentrated mass of hinge itself as well as the encompassed masses from both lateral members and diagonal members that are connected to the same hinge. Here, it is assumed that the change in m_l because of the elongation or contraction of active members on the middle plane is negligible. The reason is that this influence is much smaller compared to the other terms in Eq. (20), as will be observed later in Eq. (27).

At this point, it is of interest to have a closer look at Eq. (19). The first item of Eq. (19) describes the influence on the velocity of the ith bay because of the relative rotations of the whole bays including the ith bay itself, and the second item reflects the translation of the top plane of the ith bay that stems from the translation of each bay of the structure because of the change of its $\boldsymbol{d}$ vector. Especially, let us pay attention to the following relationship:

$$\dot{\boldsymbol{p}}_{i,k}^R = {}^A\boldsymbol{\omega}_k \times {}^A\boldsymbol{\pi}_{i,k}$$

which gives the velocity item contributed to the ith passive plane because of the relative rotation of the kth bay with an equivalent position vector $\boldsymbol{\pi}_{i,k}$. Consequently, $\boldsymbol{\pi}_{i,k}$ behaves as an equivalent rigid arm that stretches from the kth passive plane, namely, the top plane of the kth bay, to the ith passive plane.

Equation (19) can be rewritten in matrix form after substituting Eq. (13c) into it:

$$\dot{\boldsymbol{p}}_i = \sum_{k=0}^{N-1} {}_R\boldsymbol{A}_{i,k}\dot{\boldsymbol{d}}_k + \sum_{k=1}^{N} {}_T\boldsymbol{A}_{i,k}\dot{\boldsymbol{d}}_k \tag{22}$$

where

$${}_R\boldsymbol{A}_{i,k} = -{}^A\tilde{\boldsymbol{\pi}}_{i,k} {}^A\boldsymbol{P}_k \tag{22a}$$

$${}_T\boldsymbol{A}_{i,k} = {}_A\boldsymbol{D}_{j-1}(K_{ik}\boldsymbol{I} + \rho_a \boldsymbol{T}_k) \tag{22b}$$

Combining ${}_R\boldsymbol{A}_{i,k}$ and ${}_T\boldsymbol{A}_{i,k}$ into a unified form

$$\boldsymbol{A}_{i,k} = \begin{cases} {}_R\boldsymbol{A}_{i,k} & k = 0 \\ {}_R\boldsymbol{A}_{i,k} + {}_T\boldsymbol{A}_{i,k} & 0 < k < N \\ {}_T\boldsymbol{A}_{i,k} & k = N \end{cases} \tag{22c}$$

then Eq. (22) can be expressed in a more perfect form:

$$\dot{\boldsymbol{p}}_i = \boldsymbol{A}_{i,0}\dot{\boldsymbol{\Phi}}_0 + \sum_{k=1}^{N} \boldsymbol{A}_{i,k}\dot{\boldsymbol{d}}_k \tag{22d}$$

where $\boldsymbol{A}_{i,0}$ is the reaction to the ith plane from the free endplane, namely, the 0th plane. Vector $\boldsymbol{d}_k$ in the preceding equations is defined in the bay coordinate system.

IV. Angular Momentum of a VGT Structure

Here a logic bay is taken into account, and the bay coordinate system that is located on the virtual bottom plane and defined in Fig. 3 will be utilized to represent the vectors within a logic bay. A bay model with seven layers, where the first layer virtually exists, is still used to describe the geometry of a logic bay.

A. Angular Momentum of a Passive Member

As is known, the general representation of the angular momentum of a rigid member is given by

$$\boldsymbol{H}_n = \int_{\omega} \boldsymbol{r} \times \boldsymbol{v} \, \mathrm{d}m = \boldsymbol{I}_n \boldsymbol{\omega}_n + m_n \boldsymbol{g}_n \times \dot{\boldsymbol{g}}_n \tag{23}$$

For a passive member, a general case, which, as shown in Fig. 6, describes a spatial nonuniform bar, is treated here to offer a general

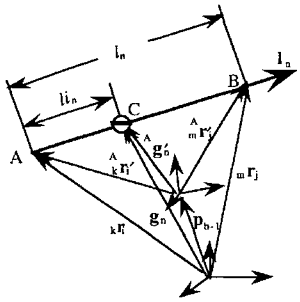

Fig. 6 Passive member.

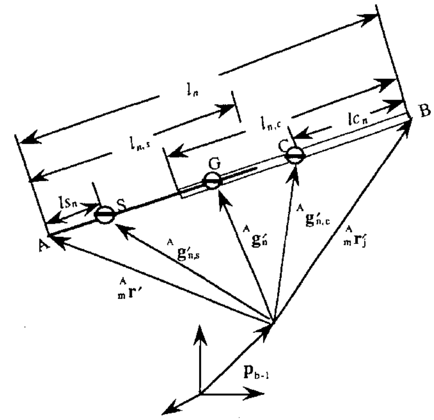

Fig. 7 Active member.

representation for computing the member's angular momentum. Assuming that its center of mass is point C, the position vectors of its two endpoints are ${}_k\boldsymbol{r}_i$ and ${}_m\boldsymbol{r}_j$, respectively, and its angular velocity with respect to an inertial coordinate system is ω_n, then the velocity distribution for an arbitrary point on it can be obtained as follows:

$$\dot{\boldsymbol{r}}_{n,s} = \dot{\boldsymbol{g}}_n + s\omega_n \times \boldsymbol{l}_n$$

Because the velocities of the two tips of the bar are ${}_k\dot{\boldsymbol{r}}_i$ and ${}_m\dot{\boldsymbol{r}}_j$, respectively, and $\omega_n \cdot \boldsymbol{l}_n = 0$, then ω_n, as well as the differentiation of $\boldsymbol{g}_n$ in the preceding equation, can be expressed as the differentiation of ${}_k\boldsymbol{r}_i$ and ${}_m\boldsymbol{r}_j$. Using Eqs. (7–9) and (12), we can obtain

$${}_j\dot{\boldsymbol{r}}_i = \dot{\boldsymbol{p}}_{b-1} + {}^A_A\omega_{b-1} \times {}^A_j\boldsymbol{r}'_i + {}_A\boldsymbol{D}_{b-1\,j}\boldsymbol{R}_i\dot{\boldsymbol{d}}_b \qquad j \in (k, m)$$

where ${}_A\boldsymbol{D}_{b-1}$ and ${}^A_A\omega_{b-1}$ describe the rotation of the bay coordinate system with respect to an inertial coordinate system [Eqs. (11) and (13c)] and $\boldsymbol{p}_{b-1}$ is the base vector of the bay coordinate system. Finally, we arrive at

$$\dot{\boldsymbol{g}}_n = \dot{\boldsymbol{p}}_{b-1} + {}^A_A\omega_{b-1} \times {}^A\boldsymbol{g}'_n + {}_A\boldsymbol{D}_{b-1}{}^+\boldsymbol{W}_n\dot{\boldsymbol{d}}_b$$

$$\omega_n = \boldsymbol{l}_n \times {}^A_A\omega_{b-1} \times \boldsymbol{l}_n + (1/l_n)\boldsymbol{l}_n \times ({}_A\boldsymbol{D}_{b-1}{}^-\boldsymbol{W}_n\dot{\boldsymbol{d}}_b)$$

where

$${}^+\boldsymbol{W}_n = [1 - (li_n/l_n)]_k\boldsymbol{R}_i + (li_n/l_n)_m\boldsymbol{R}_j \tag{24}$$

$${}^-\boldsymbol{W}_n = {}_m\boldsymbol{R}_j - {}_k\boldsymbol{R}_i \tag{24a}$$

Consequently, the angular momentum of a passive member can be expressed as

$$\boldsymbol{H}_n = m_n\boldsymbol{g}_n \times \dot{\boldsymbol{p}}_{b-1} + \boldsymbol{V}_n\dot{\boldsymbol{d}}_b + \boldsymbol{Z}_n{}^A_A\omega_{b-1} \tag{25}$$

$$\boldsymbol{V}_n = m_n\tilde{\boldsymbol{g}}_n{}_A\boldsymbol{D}_{b-1}{}^+\boldsymbol{W}_n + (\boldsymbol{I}_n/l_n)\tilde{\boldsymbol{l}}_n{}_A\boldsymbol{D}_{b-1}{}^-\boldsymbol{W}_n \tag{25a}$$

$$\boldsymbol{Z}_n = -\boldsymbol{I}_n\tilde{\boldsymbol{l}}_n\tilde{\boldsymbol{l}}_n - m_n\tilde{\boldsymbol{g}}_n{}^A\tilde{\boldsymbol{g}}'_n \tag{25b}$$

B. Angular Momentum of an Active Member

For active members of a free-floating VGT structure, a simple though very useful model is established in Fig. 7, where an active member is viewed as a compound member of two passive members. Thus, the two passive members have the same rotation with respect to the inertial reference frame and the relative translation along their common axis. It is easy to verify that Eq. (23) is still available for computing the angular momentum of active members. However, the inertial matrix $\boldsymbol{I}_n$ here must be of the compound member around its center of mass.

Assuming the two passive members of an active member to be S and C bars, respectively, then the mass center vector of the active member relative to the bay coordinate system becomes

$${}^A\boldsymbol{g}'_n = (1/m_n)\left(m_{n,s}{}^A\boldsymbol{g}'_{n,s} + m_{n,c}{}^A\boldsymbol{g}'_{n,c}\right) \tag{26}$$

where $m_{n,s}$ and $m_{n,c}$ are the masses of bar S and C, respectively. Observe that

$${}^A\boldsymbol{g}'_{n,s} = {}^A_m\boldsymbol{r}'_i + ls_n\boldsymbol{l}_n \qquad \text{and} \qquad {}^A\boldsymbol{g}'_{n,c} = {}^A_m\boldsymbol{r}'_j - lc_n\boldsymbol{l}_n$$

then substituting them into Eq. (26), after a tedious derivation, we arrive at

$${}^A\boldsymbol{g}'_n = \alpha_{n,i}{}^A_m\boldsymbol{r}'_i + \alpha_{n,j}{}^A_m\boldsymbol{r}'_j \tag{27}$$

$$\alpha_{n,i} = [1 - (m_{n,c}/m_n)] + \pi_n \quad \text{and} \quad \alpha_{n,j} = (m_{n,c}/m_n) - \pi_n \tag{27a}$$

$$\pi_n = (m_{n,c}/m_n)(lc_n/l_n) - [1 - (m_{n,c}/m_n)](ls_n/l_n) \tag{27b}$$

Moreover, differentiating Eq. (26) and noting that

$${}^A\dot{\boldsymbol{g}}'_{n,s} = {}^A_m\dot{\boldsymbol{r}}'_i + ls_n(\omega_n \times \boldsymbol{l}_n)$$

we can obtain

$${}^A\dot{\boldsymbol{g}}'_{n,s} = {}^A_m\dot{\boldsymbol{r}}'_i - (ls_n/l_n)\boldsymbol{l}_n \times \boldsymbol{l}_n \times \left({}^A_m\dot{\boldsymbol{r}}'_j - {}^A_m\dot{\boldsymbol{r}}'_i\right) \tag{28}$$

Similarly,

$${}^A\dot{\boldsymbol{g}}'_{n,c} = {}^A_m\dot{\boldsymbol{r}}_j + (lc_n/l_n)\boldsymbol{l}_n \times \boldsymbol{l}_n \times \left({}^A_m\dot{\boldsymbol{r}}_j - {}^A_m\dot{\boldsymbol{r}}'_i\right) \tag{28a}$$

With Eqs. (27), (28), and (28a), we can have

$${}^A\dot{\boldsymbol{g}}'_n = {}^A_A\omega_{b-1} \times {}^A\boldsymbol{g}'_n + {}_A\boldsymbol{D}_{b-1}{}^+\boldsymbol{W}_n\dot{\boldsymbol{d}}_b + \pi_n\boldsymbol{l}_n \times \boldsymbol{l}_n \times ({}_A\boldsymbol{D}_{b-1}{}^-\boldsymbol{W}_n\dot{\boldsymbol{d}}_b) \tag{29}$$

Substituting Eqs. (27) and (29) individually into Eq. (23), we can write the same expression as Eqs. (25) and (25b) for the angular momentum of active members with a different representation for matrix $\boldsymbol{V}_n$, which takes the form

$$\boldsymbol{V}_n = m_n\tilde{\boldsymbol{g}}_n{}_A\boldsymbol{D}_{b-1}{}^+\boldsymbol{W}_n + (\boldsymbol{I}_n/l_n)\tilde{\boldsymbol{l}}_n{}_A\boldsymbol{D}_{b-1}{}^-\boldsymbol{W}_n + m_n\pi_n\tilde{\boldsymbol{g}}_n\tilde{\boldsymbol{l}}_n\tilde{\boldsymbol{l}}_n{}_A\boldsymbol{D}_{b-1}{}^-\boldsymbol{W}_n \tag{30}$$

where ${}^-\boldsymbol{W}_n$ takes the same form as Eq. (24a) and ${}^+\boldsymbol{W}_n$ is found by

$${}^+\boldsymbol{W}_n = [1 - (m_{n,c}/m_n)]_k\boldsymbol{R}_i + (m_{n,c}/m_n)_m\boldsymbol{R}_j \tag{31}$$

C. Total Angular Momentum of a Bay

The total angular momentum $\boldsymbol{H}_b$ of a virtual bay can be obtained by summing up the angular momentum of those components just derived and can be represented as

$$\boldsymbol{H}_b = M_b\boldsymbol{g}_b \times \dot{\boldsymbol{p}}_{b-1} + \boldsymbol{V}_b\dot{\boldsymbol{d}}_b + \boldsymbol{Z}_b{}^A_A\omega_{b-1} \tag{32}$$

where matrix $\boldsymbol{V}_b$ stands for the contribution to $\boldsymbol{H}_b$ resulting from the change of vector $\boldsymbol{d}_b$ of a bay and therefore governed by the geometric and physical properties of the bay itself; $\boldsymbol{Z}_b$ then shows the coupling effects with the other bays through the rotations of those bay coordinate systems.

D. Total Angular Momentum of the Structure

Upon the substitution of Eqs. (13c) and (22d) into Eq. (32) and the summation of the angular momentum of all bays of the structure, we are able to obtain the total angular momentum $\boldsymbol{H}$

$$\boldsymbol{H} = \boldsymbol{H}_0 \dot{\boldsymbol{\Phi}}_0 + \sum_{b=1}^{N} \boldsymbol{H}_b \dot{\boldsymbol{d}}_b \tag{33}$$

$$\boldsymbol{H}_0 = \left(\sum_{b=0}^{N} \boldsymbol{Z}_b \right) \boldsymbol{P}_0 + M_0 \tilde{\boldsymbol{p}}_0 \boldsymbol{A}_{0,0} + \sum_{b=1}^{N} M_b \tilde{\boldsymbol{g}}_b \boldsymbol{A}_{b-1,0} \tag{33a}$$

$$\boldsymbol{H}_j = M_0 \tilde{\boldsymbol{p}}_0 \boldsymbol{A}_{0,j} + \boldsymbol{V}_j + \sum_{b=1}^{N} M_b \tilde{\boldsymbol{g}}_b \boldsymbol{A}_{b-1,j} + \left(\sum_{b=j+1}^{N} \boldsymbol{Z}_b \right) {}^{A}\boldsymbol{P}_j \tag{33b}$$

E. Conservation of Momentum

In the preceding sections, we presented both the position and the corresponding velocity governing equations (18) and (22d), as well as the orientation and angular velocity control equations (11) and (13c). In the course of deriving Eq. (18), the integral form of the conservation of translation momentum has been used with an implicit assumption: the structure is set in a conservative dynamic system and is initially static. Note that these equations alone are unable to describe the structural motion completely. In fact, there is still no way to relate the orientations of two free endplanes of a free-floating VGT structure, which could be provided by the law of conservation of angular momentum of the structure system.

When a VGT structure is in a completely free-floating state, in which no external force is applied, Eq. (33) becomes

$$\boldsymbol{H}_0 \dot{\boldsymbol{\Phi}}_0 + \sum_{b=1}^{N} \boldsymbol{H}_b \dot{\boldsymbol{d}}_b = \text{const} \tag{34}$$

If the structure is still assumed to be initially static, const will be zero, so that

$$\dot{\boldsymbol{\Phi}}_0 = -\sum_{b=1}^{N} \boldsymbol{H}_0^{-1} \boldsymbol{H}_b \dot{\boldsymbol{d}}_b \tag{35}$$

V. Simulation

To test the validity of the equations derived in this paper and with the aim of future applications of adaptive structures to space construction, an object-oriented program system VGTMOT[10] is developed to perform the digital simulation and practical experiment control for a VGT set in the laboratory (Fig. 1). There are many potential applications for the equations proposed in this paper. Here, the computer simulation is carried out for a significant application of free-floating structures, namely, the docking problem raised in the introduction. The computing model comes from a practical four bays' VGT structure, whose specifications are listed in the Tables 1 and 2.

Assume that the structure is in a fully packed preliminary state and the origin of an inertial coordinate system is set to coincide with the center of mass of the structure (Fig. 8). The position of the docking target is specified in Table 3. First, a prepared deployment of the structure along the Y axis is done to make the docking endplane enter to the region of the docking plane. Then, through maneuvering both the center of mass and the orientation of the right endplane, as shown in Fig. 8, by a prespecified trajectory, if the time step is set to be 0.3 s, then after 23 steps the endplane succeeds in reaching the docking port accurately. The resolved motion rate control approach is used to achieve control, and the Moore–Penrose inverse is used to solve the inverse kinematics. The shape changing procedure and the final shape of the structure are illustrated in Fig. 9 with vector $\boldsymbol{d}$ of each bay. The altering procedure of the orientation of the free endplane is shown in Fig. 10.

Table 1 Specification of the computing model

	Total structure	Diagonal passive member	Lateral passive member	Hinge
Weight, kg	23.13	0.04	0.74	0.05
Length, mm		400	400	
li		200	158	
Δ				16

Table 2 Specification of active members

	Weight, kg	Length, mm	li[a]	Maximal length	Minimal length
Compound bar	0.73			620	400
Left bar	0.5	356	155		
Right bar	0.23	334	262		

[a]Here li corresponds to ls for the left bar and lc for the right bar, respectively (Fig. 7).

Table 3 Position specification of docking target

Position of mass center of docking plane			Orientation of docking plane (Euler angles, deg)		
X	Y	Z	Φ	Θ	Ψ
−5.67	−1217.3	154.3	59.40	0.2	0.0

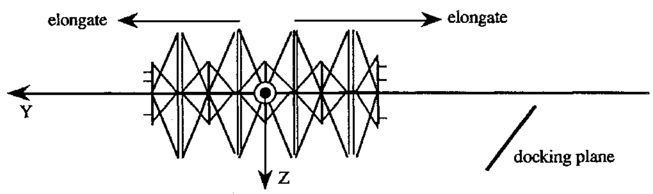

Fig. 8 Installation of docking mechanism.

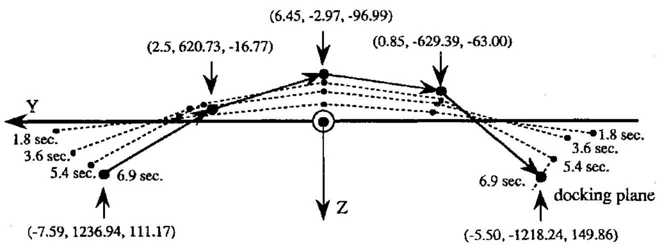

Fig. 9 Docking procedure.

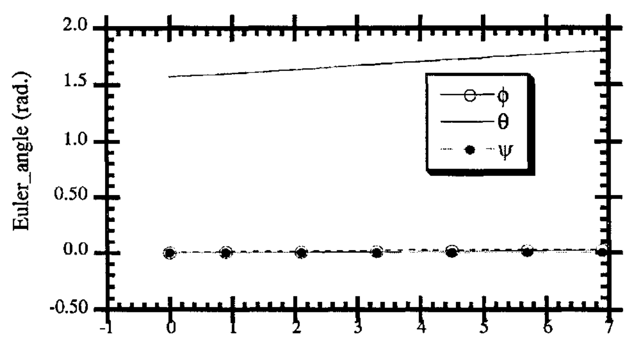

Fig. 10 Orientation-time curve of the free endplane.

VI. Conclusions

An alternate application for a variable geometry truss is proposed. With the aim of their realization in future space construction, the kinematics of a free-floating variable geometry truss are investigated, and a family of compact equations describing its motion control in three-dimensional space is formulated on the basis of the conservation of momentum of the structural system and the centroid displacement vector $\boldsymbol{d}$ of a bay. To test the validity of the derived equations, a simulation of a docking control for a free-floating variable geometry truss is carried out.

Appendix: Relative Angular Velocity of a Bay

A. Basic Operations on Vectors and Skew Matrices

If $\boldsymbol{a} = \{a_1, a_2, a_3\}$ is a direction vector, i.e., $\boldsymbol{a}^T\boldsymbol{a} = 1$, then we can have

$$\tilde{\boldsymbol{a}}\tilde{\boldsymbol{a}} + \boldsymbol{I} = \boldsymbol{a}\boldsymbol{a}^T \tag{A1}$$

For arbitrary vectors $\boldsymbol{a}$, $\boldsymbol{b}$, and $\boldsymbol{c}$, we can establish the following relationships:

$$\tilde{\boldsymbol{a}}\tilde{\boldsymbol{b}} = \boldsymbol{b}\boldsymbol{a}^T - (\boldsymbol{a}^T\boldsymbol{b})\boldsymbol{I} \tag{A2}$$

$$\text{if} \quad \boldsymbol{c} = \boldsymbol{b}\times\boldsymbol{a}, \quad \text{then} \quad \tilde{\boldsymbol{c}} = \boldsymbol{a}\boldsymbol{b}^T - \boldsymbol{b}\boldsymbol{a}^T \tag{A3}$$

B. Derivation of the Relative Angular Velocity of a Bay

Before we begin to derive the angular velocity of a bay, some necessary results are needed, which are obtained by differentiating Eqs. (1a) and (1c) expressed as

$$\frac{\mathrm{d}(\cos\varphi)}{\mathrm{d}t} = 2\frac{\boldsymbol{d}^T\boldsymbol{n}_1}{\boldsymbol{d}^T\boldsymbol{d}}(\boldsymbol{n}_1 - \boldsymbol{n}_2)\dot{\boldsymbol{d}} \tag{A4}$$

$$\frac{\mathrm{d}(\boldsymbol{v}\boldsymbol{v}^T)}{\mathrm{d}t} = \frac{1}{\|\boldsymbol{d}\times\boldsymbol{n}_1\|}\Big\{(\dot{\boldsymbol{d}}\times\boldsymbol{n}_1)\boldsymbol{v}^T + \boldsymbol{v}(\dot{\boldsymbol{d}}\times\boldsymbol{n}_1)^T - 2\big[\boldsymbol{v}^T(\dot{\boldsymbol{d}}\times\boldsymbol{n}_1)\big]\boldsymbol{v}\boldsymbol{v}^T\Big\} \tag{A5}$$

We know that the relative angular velocity of a bay has been defined to be [Eq. (4)]

$$\tilde{\omega} = \dot{\boldsymbol{D}}_b\boldsymbol{D}_b^T$$

Differentiating Eq. (1), we obtain

$$\dot{\boldsymbol{D}}_b = \frac{\mathrm{d}(\cos\varphi)}{\mathrm{d}t}(\boldsymbol{I} - \boldsymbol{v}\boldsymbol{v}^T + ctg\varphi\cdot\boldsymbol{v}^T) - \sin\varphi\cdot\frac{\mathrm{d}\boldsymbol{v}}{\mathrm{d}t} + \frac{1-\cos\varphi}{\|\boldsymbol{d}\times\boldsymbol{n}_1\|}\Big\{(\dot{\boldsymbol{d}}\times\boldsymbol{n}_1)\boldsymbol{v}^T + \boldsymbol{v}(\dot{\boldsymbol{d}}\times\boldsymbol{n}_1)^T - 2\big[\boldsymbol{v}^T(\dot{\boldsymbol{d}}\times\boldsymbol{n}_1)\big]\boldsymbol{v}\boldsymbol{v}^T\Big\} \tag{A6}$$

Let

$$\dot{\boldsymbol{D}}_b\boldsymbol{D}_b^T = \boldsymbol{I}_1 + \boldsymbol{I}_2 - \boldsymbol{I}_3$$

where

$$\boldsymbol{I}_1 = \frac{\mathrm{d}(\cos\varphi)}{\mathrm{d}t}(\boldsymbol{I} - \boldsymbol{v}\boldsymbol{v}^T + ctg\varphi\cdot\boldsymbol{v}^T)[\cos\varphi\boldsymbol{I} + (1-\cos\varphi)\boldsymbol{v}\boldsymbol{v}^T + \sin\varphi\tilde{\boldsymbol{v}}]\frac{1}{\sin\varphi}\frac{\mathrm{d}(\cos\varphi)}{\mathrm{d}t}\tilde{\boldsymbol{v}}$$

$$\boldsymbol{I}_2 = \frac{1-\cos\varphi}{\|\boldsymbol{d}\times\boldsymbol{n}_1\|}\Big\{(\dot{\boldsymbol{d}}\times\boldsymbol{n}_1)\boldsymbol{v}^T + \boldsymbol{v}(\dot{\boldsymbol{d}}\times\boldsymbol{n}_1)^T - 2[\boldsymbol{v}^T(\dot{\boldsymbol{d}}\times\boldsymbol{n}_1)]\boldsymbol{v}\boldsymbol{v}^T\Big\}[\cos\varphi\boldsymbol{I} + (1-\cos\varphi)\boldsymbol{v}\boldsymbol{v}^T + \sin\varphi\tilde{\boldsymbol{v}}]$$

$$\boldsymbol{I}_3 = \sin\varphi\cdot\frac{\mathrm{d}\boldsymbol{v}}{\mathrm{d}t}[\cos\varphi\boldsymbol{I} + (1-\cos\varphi)\boldsymbol{v}\boldsymbol{v}^T + \sin\varphi\tilde{\boldsymbol{v}}]$$

Then after a tedious simplification, we can arrive at

$$\omega = \frac{1}{\|\boldsymbol{d}\times\boldsymbol{n}_1\|}((1-\cos\varphi)[\boldsymbol{v}\times(\dot{\boldsymbol{d}}\times\boldsymbol{n}_1)] + \sin\varphi\{\boldsymbol{v}\times[\boldsymbol{v}\times(\dot{\boldsymbol{d}}\times\boldsymbol{n}_1)]\}) + \frac{1}{\sin\varphi}\frac{\mathrm{d}(\cos\varphi)}{\mathrm{d}t}\boldsymbol{v} \tag{A7}$$

Substituting Eqs. (1a), (1c), and (A4) into Eq. (A7) and noting that vector $\boldsymbol{n}_1 = (0, 0, 1)$ in the bay coordinate system, finally we can obtain Eq. (5).

References

[1] Wada, B. K., Fanson, J., and Crawley, E., "Adaptive Structure," *Journal of Intelligent Material Systems and Structures*, Vol. 1, April 1990, pp. 157–174.

[2] Natori, M. C., "Outline of Space Structure Engineering," *Proceedings of the JSCE*, No. 398/I-10, Japan Society of Civil Engineering, Tokyo, Japan, 1989, pp. 1–16 (in Japanese).

[3] Miura, K., and Furuya, H., "Adaptive Structure Concept for Future Space Applications," *AIAA Journal*, Vol. 26, No. 8, 1988, pp. 995–1002.

[4] Tidwell, P. H, Reinholtz, C. F., Robertshaw, H. H., and Horner, C. G., "Kinematic Analysis of Generalized Adaptive Trusses," *First Joint U.S./Japan Conference on Adaptive Structures* (Maui, HI), Technomic, Lancaster, PA, 1990, pp. 772–791.

[5] Naccarato, F., and Hughes, P., "Redundancy Resolution in Variable-Geometry Truss Manipulators Using Reference Shape Curves," *Second Joint U.S./Japan Conference on Adaptive Structures* (Nagoya, Japan), Technomic, Lancaster, PA, 1991, pp. 539–555.

[6] Umetani, Y., and Yoshida, K., "Resolved Motion Rate Control of Space Manipulators with Generalized Jacobian Matrix," *IEEE Transactions on Robotics and Automation*, Vol. 5, No. 3, 1989, pp. 303–314.

[7] Matunaga, S., "On the Construction of Large Space Structure Using Intelligent/Adaptive Structure," Ph.D. Thesis, Div. of Engineering, Graduate School, Tokyo Univ., Tokyo, Japan, Dec. 1990.

[8] Shabana, A. A., *Dynamics of Multibody Systems*, Wiley-Interscience, New York, 1989.

[9] Chiou, J. C., "Constraint Treatment Techniques and Parallel Algorithms for Multibody Dynamics Analysis," Ph.D. Thesis, Center for Space Structures and Control, Univ. of Colorado, CU-CSSC-90-26, Boulder, CO, Nov. 1990.

[10] Huang, S. Y., Natori, M. C., Nakai, S., and Katukura, H., "An Object-Oriented Approach to the Motion Control of a Free-Floating Variable Geometry Truss," *Proceedings of the AIAA/ASME/ASCE/AHS/ASC 35th Structures, Structural Dynamics, and Materials Conference and the AIAA/ASME Adaptive Structures Forum*, AIAA, Washington, DC, 1994, pp. 465–473.